



Alfred Wegener Institute
for Polar and Marine Research

Ocean state in the last decade determined by 4-D VAR data assimilation

J. Staneva, M. Wenzel and J. Schröter

Alfred Wegener Institute for Polar and Marine Research, Bremerhaven, Germany



The Problem

The ocean data assimilation is directed towards the combined use of ocean models and data aiming to improve the model representation of a time dependent oceanic state. The main purpose of this study is to obtain an oceanic state over the last decade consistent with ocean observations. The impact of combining the different surface and subsurface data on the simulated ocean state is studied using the Hamburg Large Scale Geostrophic (LSG) model. It is a coarse resolution OGCM ($3.5^\circ \times 3.5^\circ$ in the horizontal and 11 vertical levels) originally designed for climate studies. The implicit formulation in time of the LSG allows for a time step of one month. The assimilation technique is based on adjoint method. As a reference run, the LSG model is forced subsequently with monthly data from the NCEP reanalyses project for 1950-2001. We will further refer to this as reference run **REF**. The oceanic state determined by **REF** is compared to the results from an optimized solution (**OPT**), in which the model is fitted to nine years (1993-2001) of TOPEX/POSEIDON (T/P) anomalies. Additionally we utilize the same data sets as in Wenzel et al. (2001) but with reduced weights. As control parameters for the optimization we use the model initial temperature and salinity state as well as the mean annual cycle of the wind stress, air temperature and freshwater flux, while the additional temporal variability of the forcing is taken from the NCEP reanalysis.

Method

In the adjoint assimilation technique the misfit between the data and corresponding model counterparts is formulated in a cost function \mathbf{J} which is minimized. Via the model equations, which must be fulfilled exactly, the cost function depends implicitly on a set of parameters or control variables $\{X_i\}$.

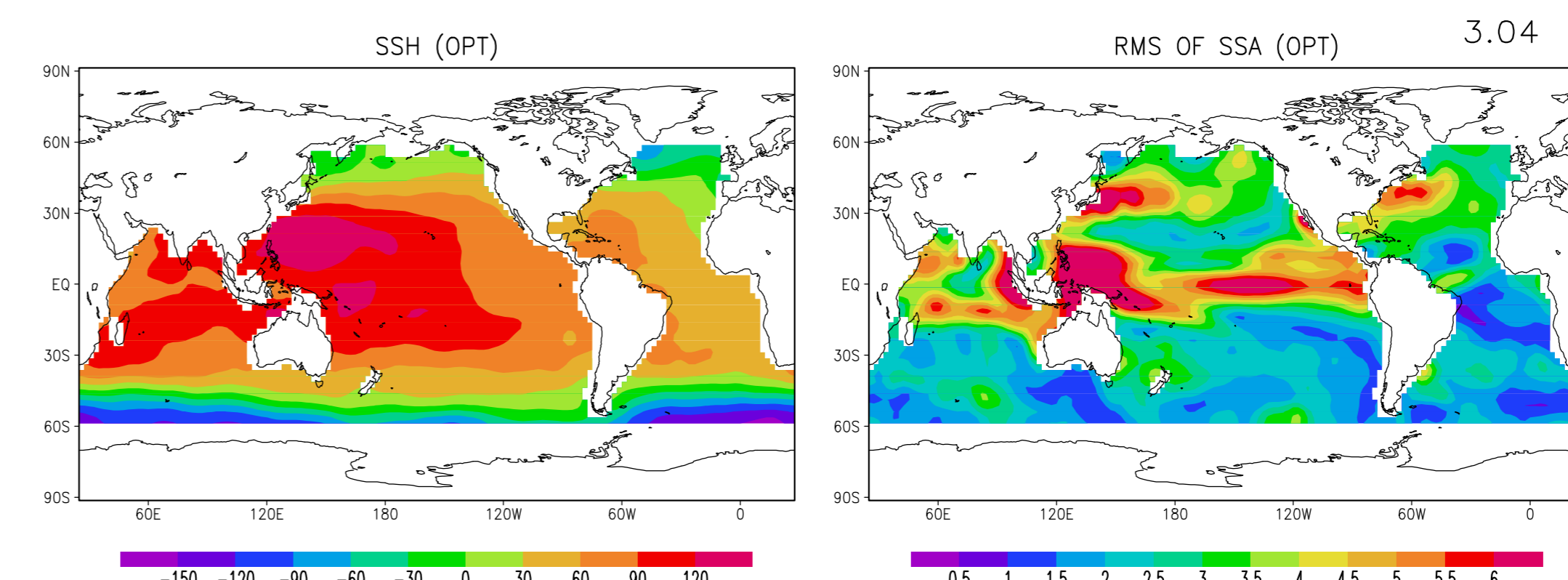
⇒ Here we solve for the initial conditions as well as the mean forcing (monthly wind stress, air temperature and freshwater fluxes), which provide the best model-data comparisons. Because of the different adjustment time scales involved, the model state for the upper ocean is mainly influenced by the forcing, while the deep ocean remains close to the initial state for short times of integration. In order to adjust both the upper and the deep ocean we use the same procedure described by Wenzel et al. (2001). We split the assimilation procedure into two parts and apply the following strategy:

⇒ First we perform ten years assimilation to improve initial state for temperature, salinity and sea surface elevation.

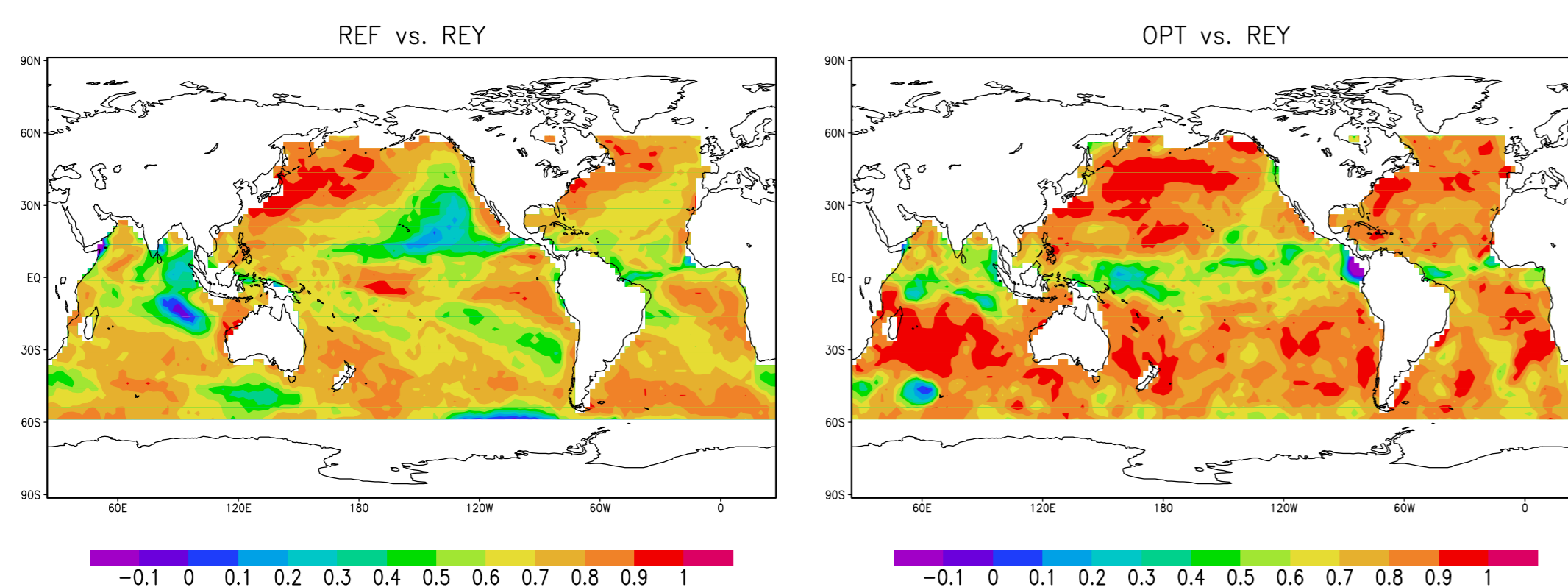
The control variables are reduced to only the initial conditions for the potential temperature, salinity and the sea surface elevation for January, 1992. Velocities are taken from their first guess values. The cost function \mathbf{J}_1 covers only the last nine years (1993-2001) while 1992 is used to let the velocities adjust to the optimized density structure.

⇒ Once the minimum of \mathbf{J}_1 has been found we perform another assimilation to find better monthly forcing fields.

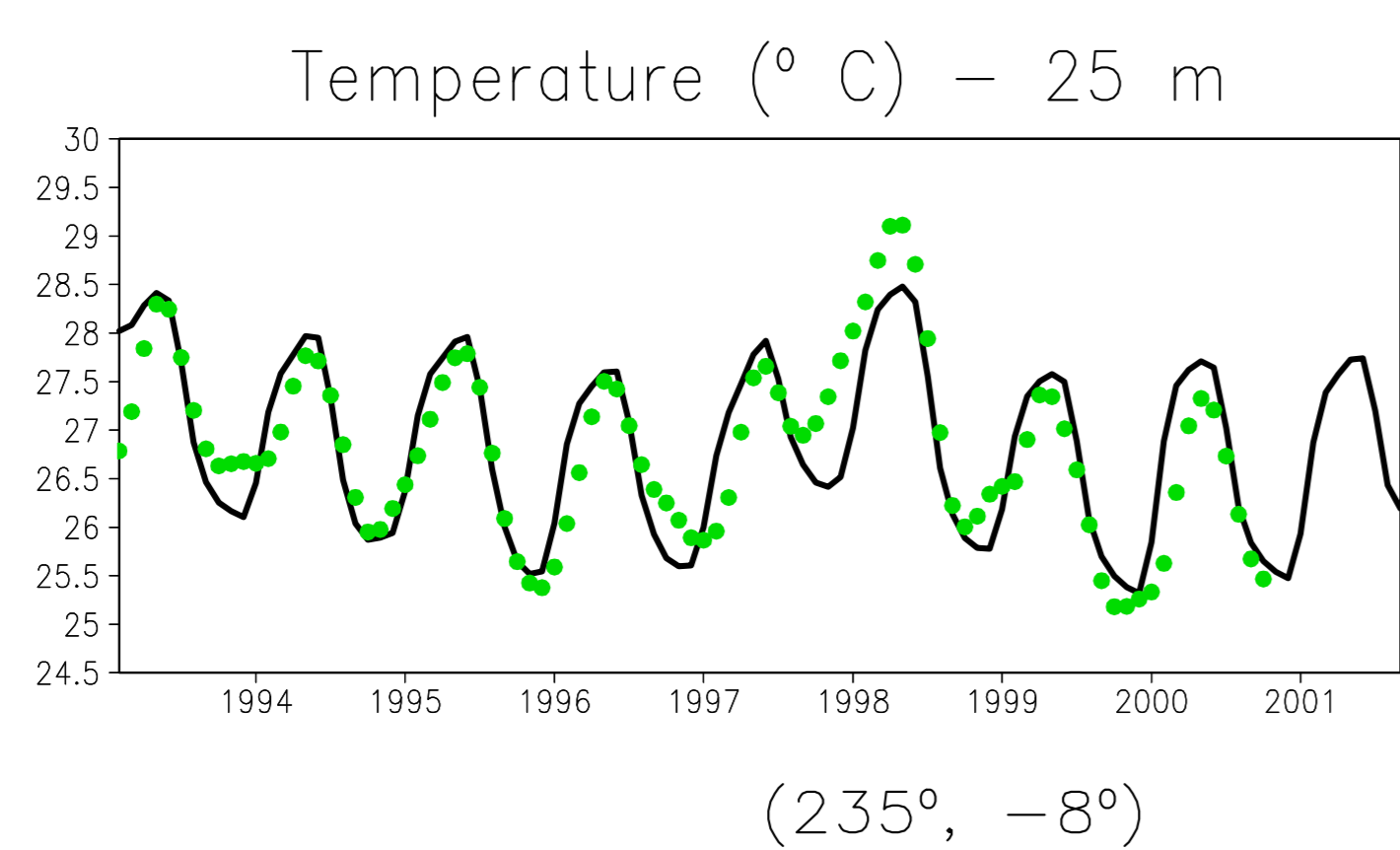
To start this two optimization cycles, which minimize the cost functions \mathbf{J}_1 and \mathbf{J}_2 , we need a first guess initial model state and forcing fields. It is taken from the optimized solution obtained by Staneva et al. (2002) in which a hierarchy of seven-year (1993-1999) assimilation experiments have been done. After improving the initial state, January values of the optimal integration are used as initial state in minimizing \mathbf{J}_2 .



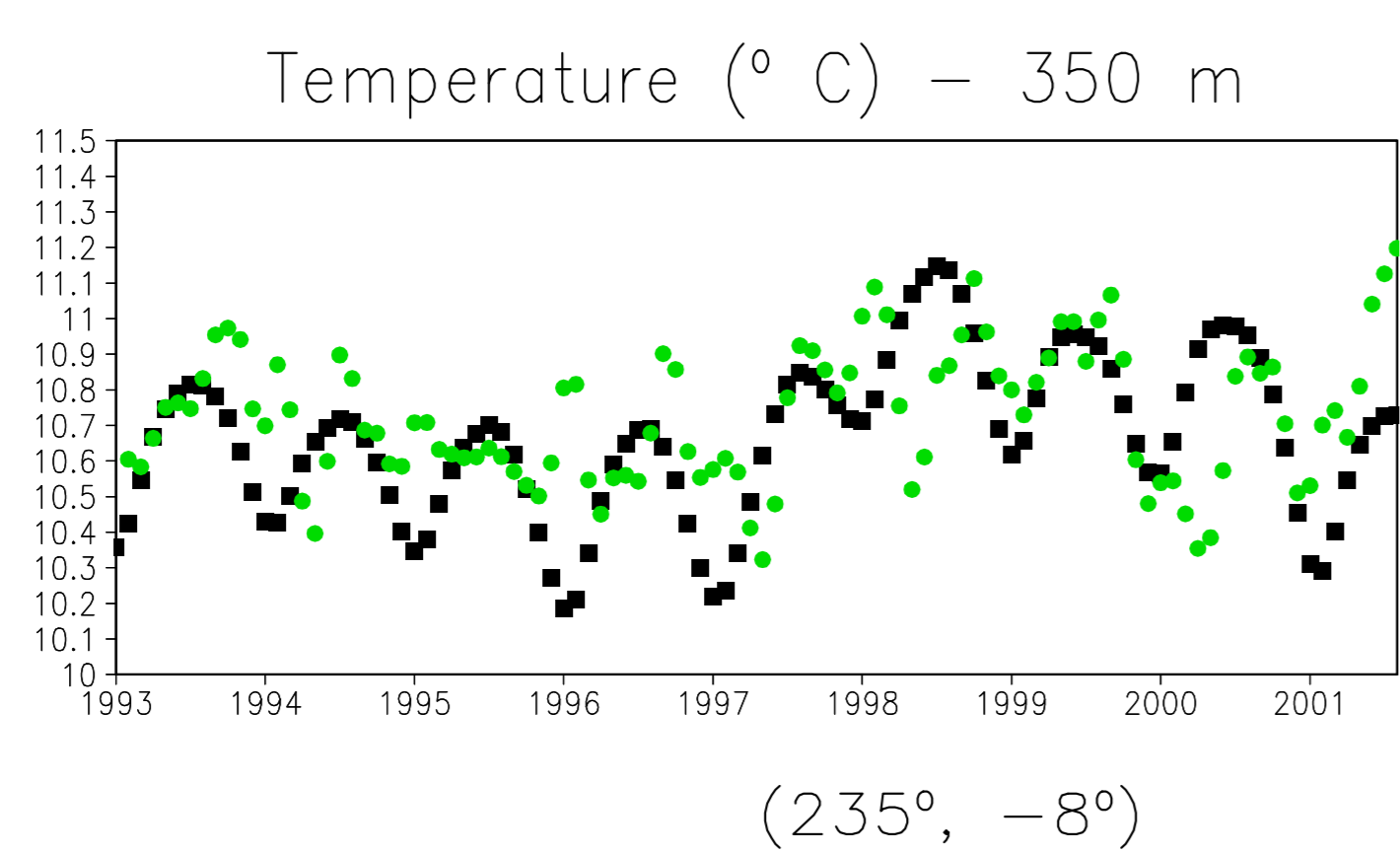
Nine-year mean SSH from the optimized solution (left); RMS variability of the sea surface anomaly from **OPT** (right). The units are in cm. The total variability is given on the top right corner.



Nine years mean correlation of Sea Surface Temperature [°C] between **REF** and Reynolds data (left) as well as between **OPT** and Reynolds data (right).

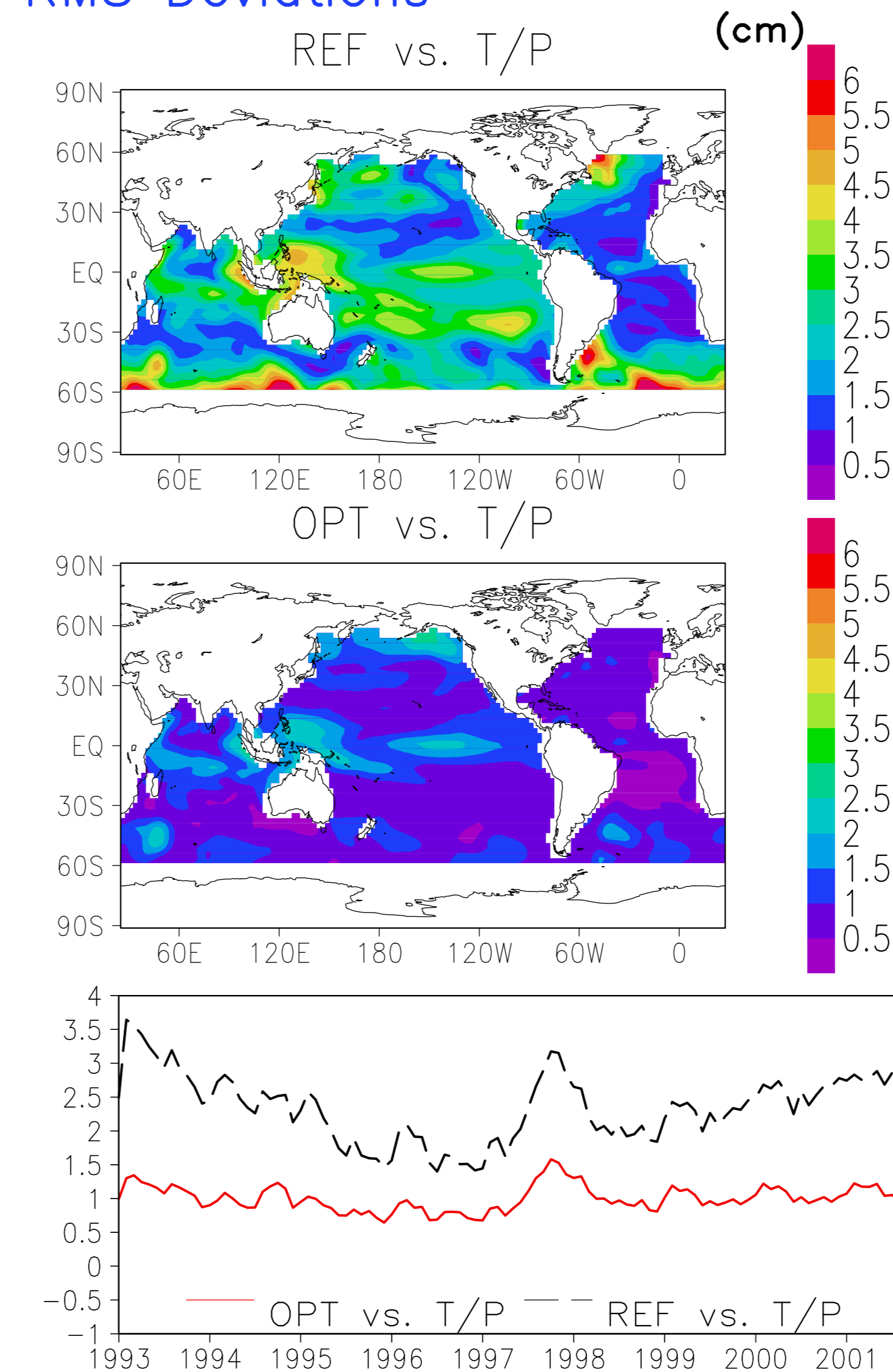


Time series of temperature [°C] obtained from the nine-year model simulations **OPT** and Tropical Atmosphere Ocean (TAO) data at 25 m.



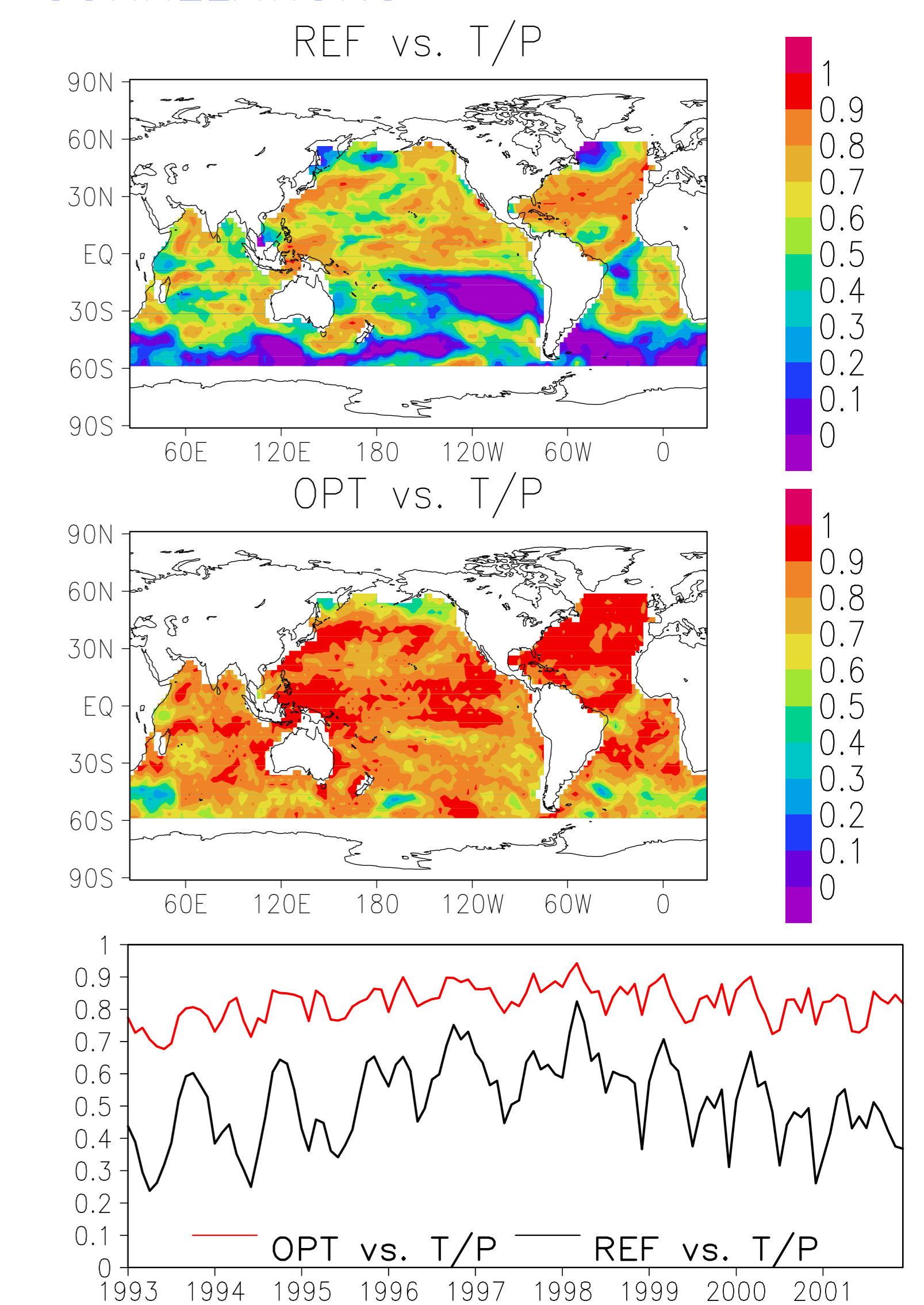
Time series of temperature [°C] obtained from the nine-year model simulations **OPT** and TAO data at 350 m.

RMS Deviations

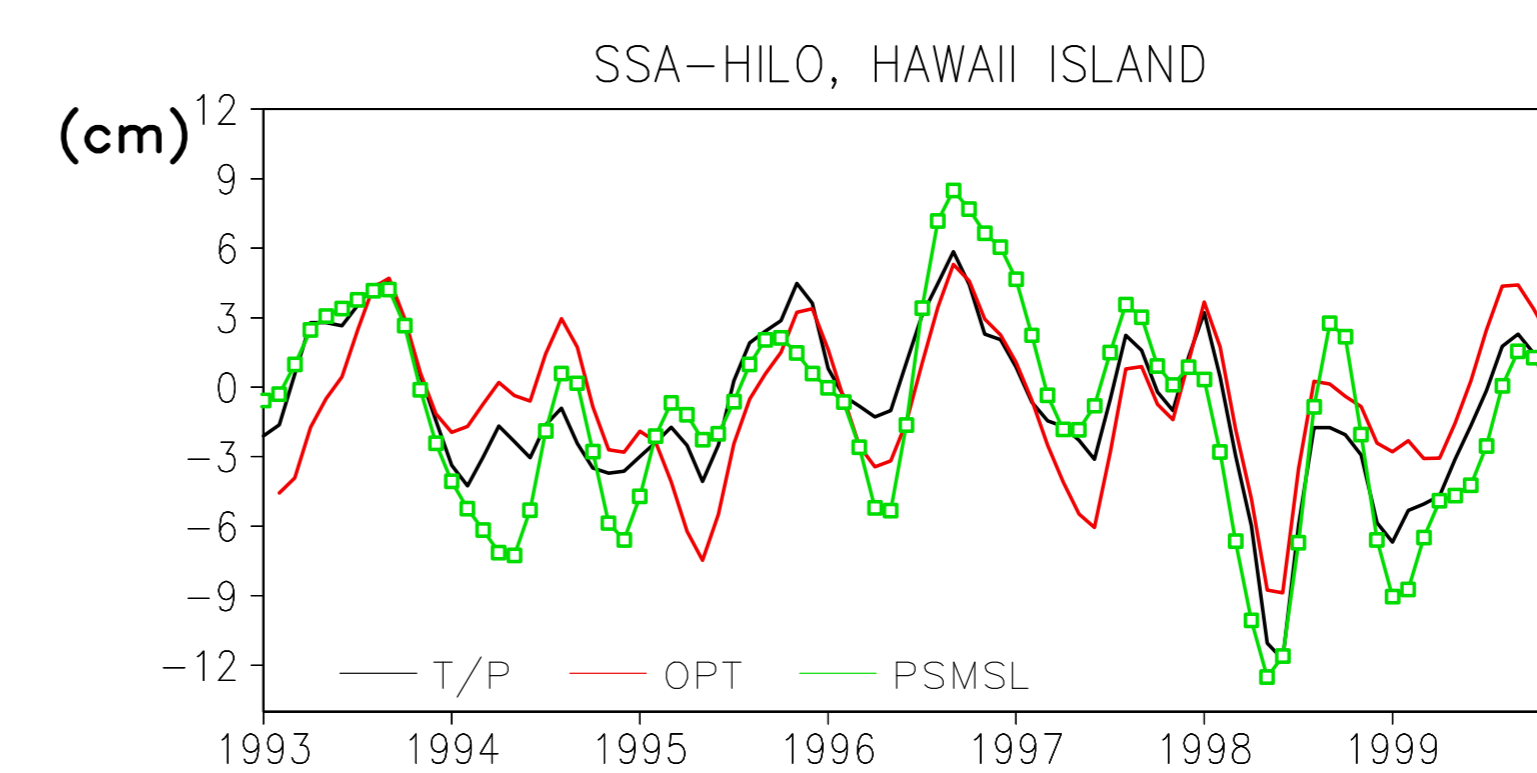


RMS deviations of the SSA from the T/P data for the reference run **REF** (top) and the optimal solution **OPT** (middle). The bottom figure shows the area mean RMS deviation as a function of time. The units are in cm. The model improvements in simulating the observed TOPEX/POSEIDON sea level variability by the assimilation is clearly seen.

CORRELATIONS



Temporal mean correlation of SSA between **REF** and T/P (top) as well as between **OPT** and T/P data (middle). The area mean correlations as a function of time are shown at the bottom pattern.

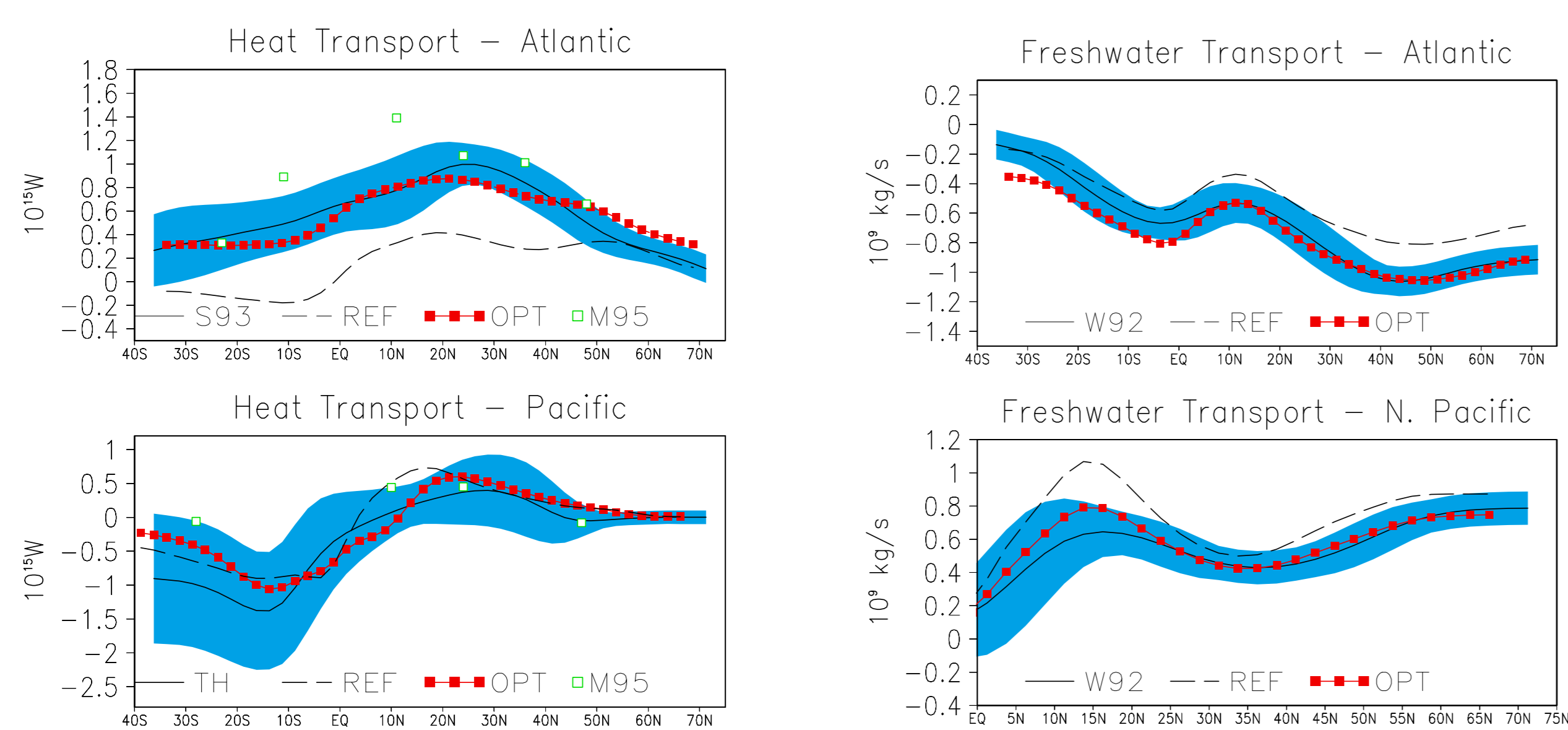


Comparisons of sea level of T/P altimetry data (black) and model simulations (red) with tide gauge data at Hilo, Hawaii Island (green). The values are temporal anomalies of the respective estimates. The units are in cm.

The Ocean State

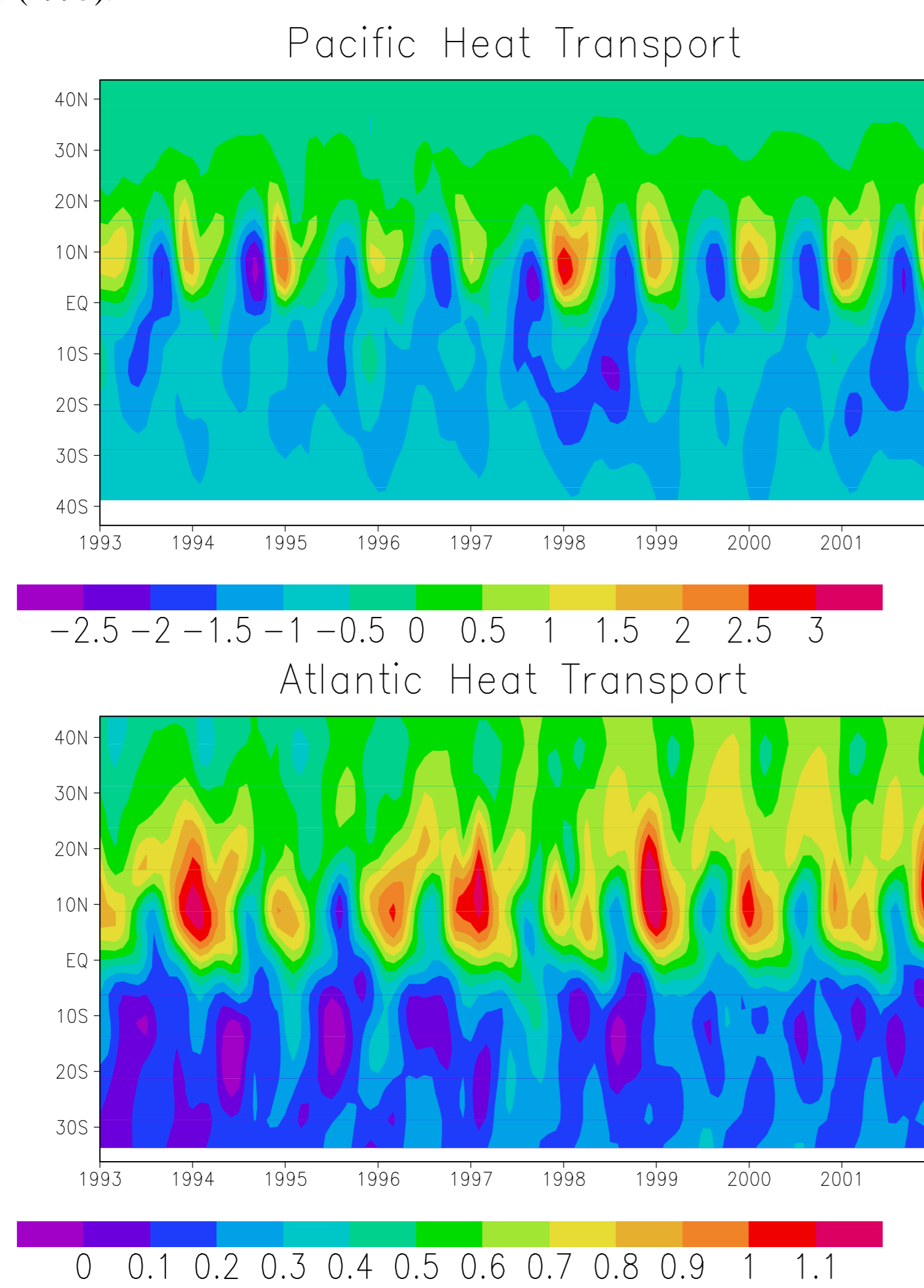
The assimilation results demonstrate the improvement of the model capabilities of the constrained model in comparison with the reference one to predict the variability of the ocean circulation and heat and freshwater transports. The errors between the model and the data are significantly reduced, except in the equatorial Pacific and ACC. The horizontal patterns of SSA of T/P altimetry data are quite similar to that obtained by the constrained model. The largest differences between the variability of the altimetry data and model simulations are observed in the equatorial Pacific and Indian oceans. The deviations of the SSA variability obtained by the constrained model from that of the T/P anomalies are better pronounced in the regions of the strong currents. The latter indicates that the model transports in the optimized solution are still weaker even though significantly improved with respect to the hindcast experiment.

The differences between the temperature estimated by the constrained model and the temperature taken from the Levitus climatology and WOCE data are shown as well. The WOCE hydrography and Levitus data are interpolated to the model grid, therefore all small scale structures related to the eddies in the WOCE hydrography are eliminated. The large-scale structures simulated by the model are in visually good agreement with the data. The differences are mainly pronounced in the upper layers. The deviations obtained by the constrained model clearly indicate the model deficits due to its coarse horizontal resolution. It is seen from the vertical sections that the temperature of the assimilation experiment compares better to the independent temperature of the WOCE sections than to the Levitus climatology, indicating that the model stratification tends to be closer to the real hydrographical data rather than to the climatological ones. Giving most weight to the constraints on sea surface height improves the density of the model to a structure more realistic than climatology.

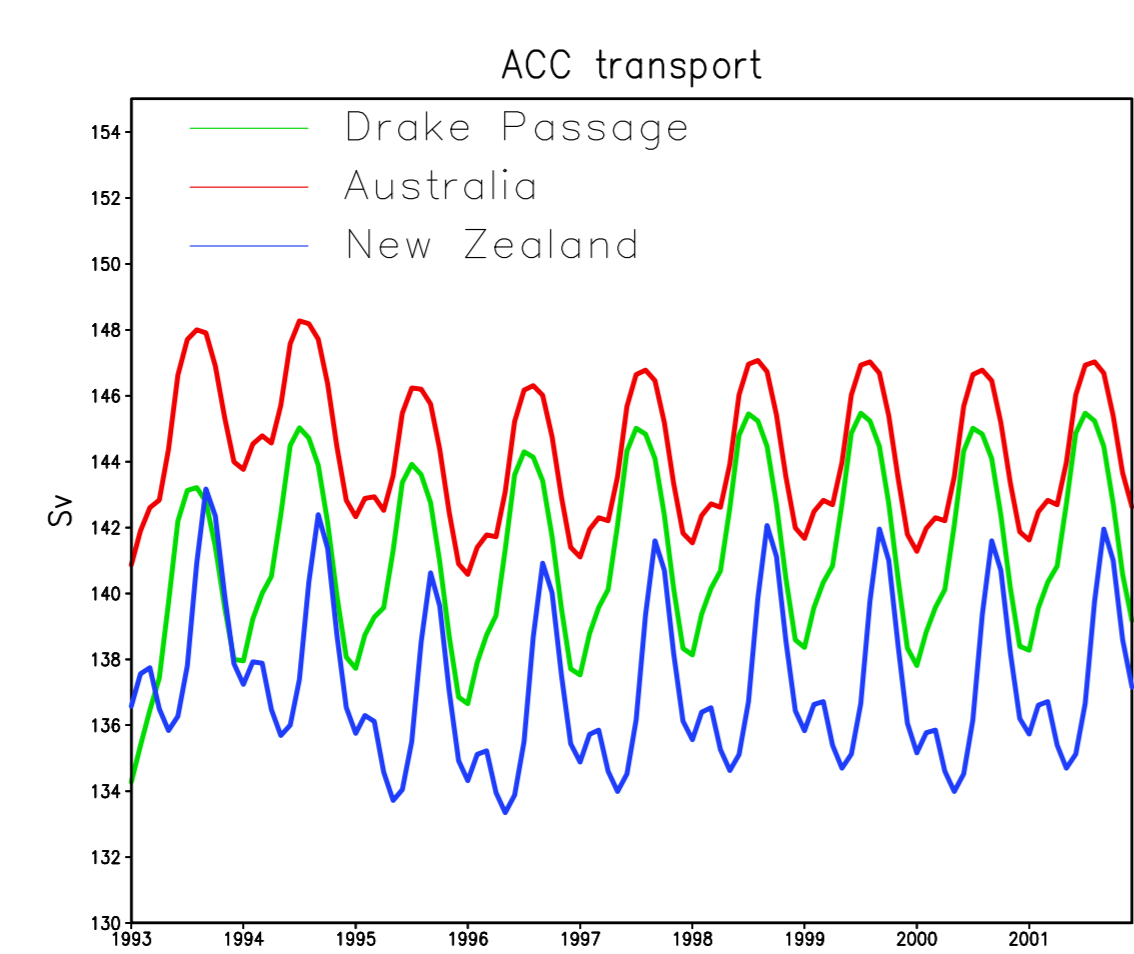


Temporal mean meridional heat transport [10^{15} W]. Red line with squares-from **OPT**, black dash line-from **REF**; black full line-data compiled from various estimates e.g. Schlitzer, 1993 (S93) for Atlantic and Talley, 1984 and Hsiung, 1985 (TH) for Pacific with error bars (blue shading); green squares: data from Macdonald (1995).

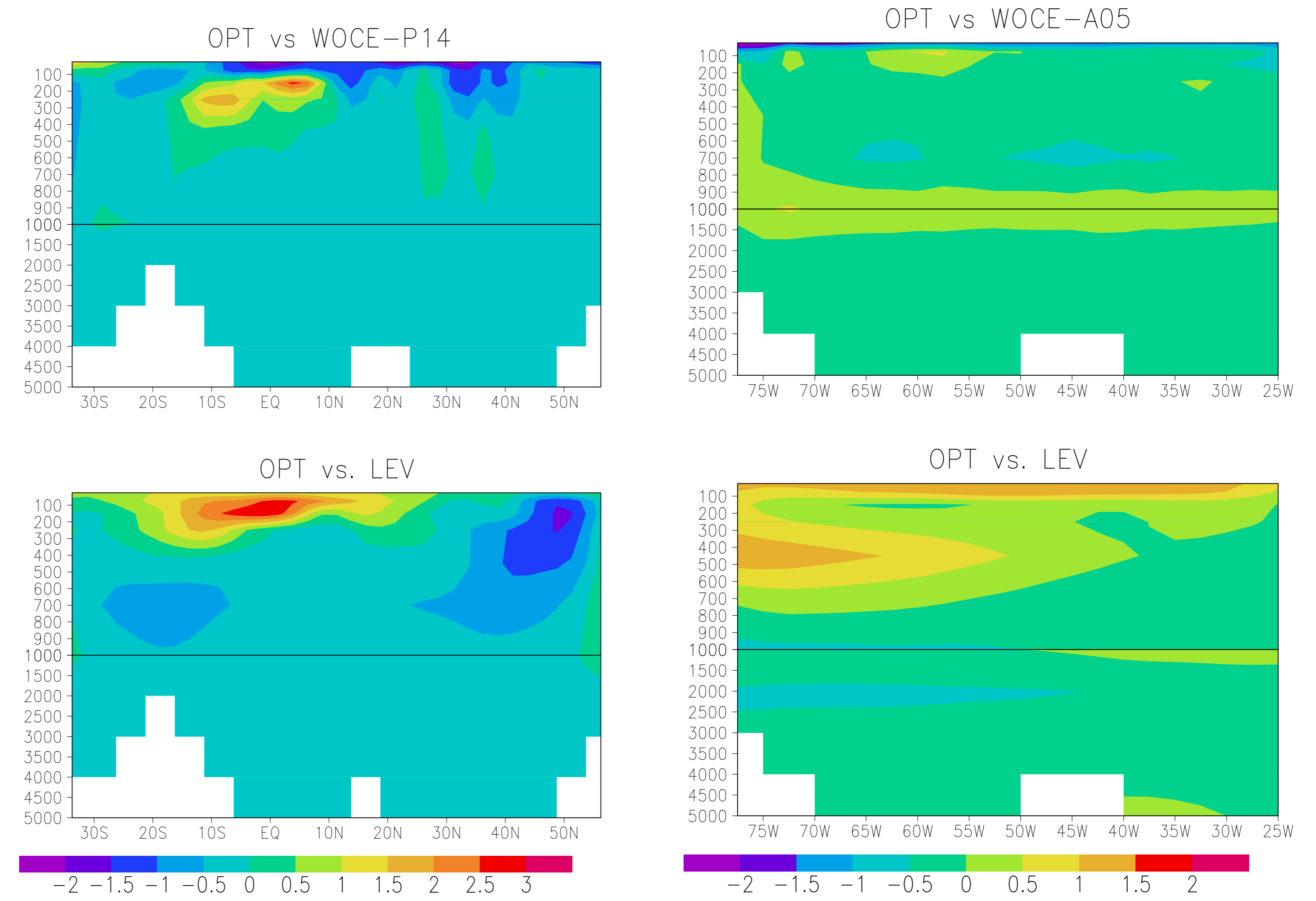
Temporal mean meridional freshwater transport. Red line-from **OPT**, black dash line-from **REF**, black full line-data given by Wijffels et al, 1992 (W92) with error bars (blue shading).



Latitude-time sections of the Pacific (top) and the Atlantic (bottom) meridional heat transport [10^{15} W] from the nine year optimal solution **OPT**.

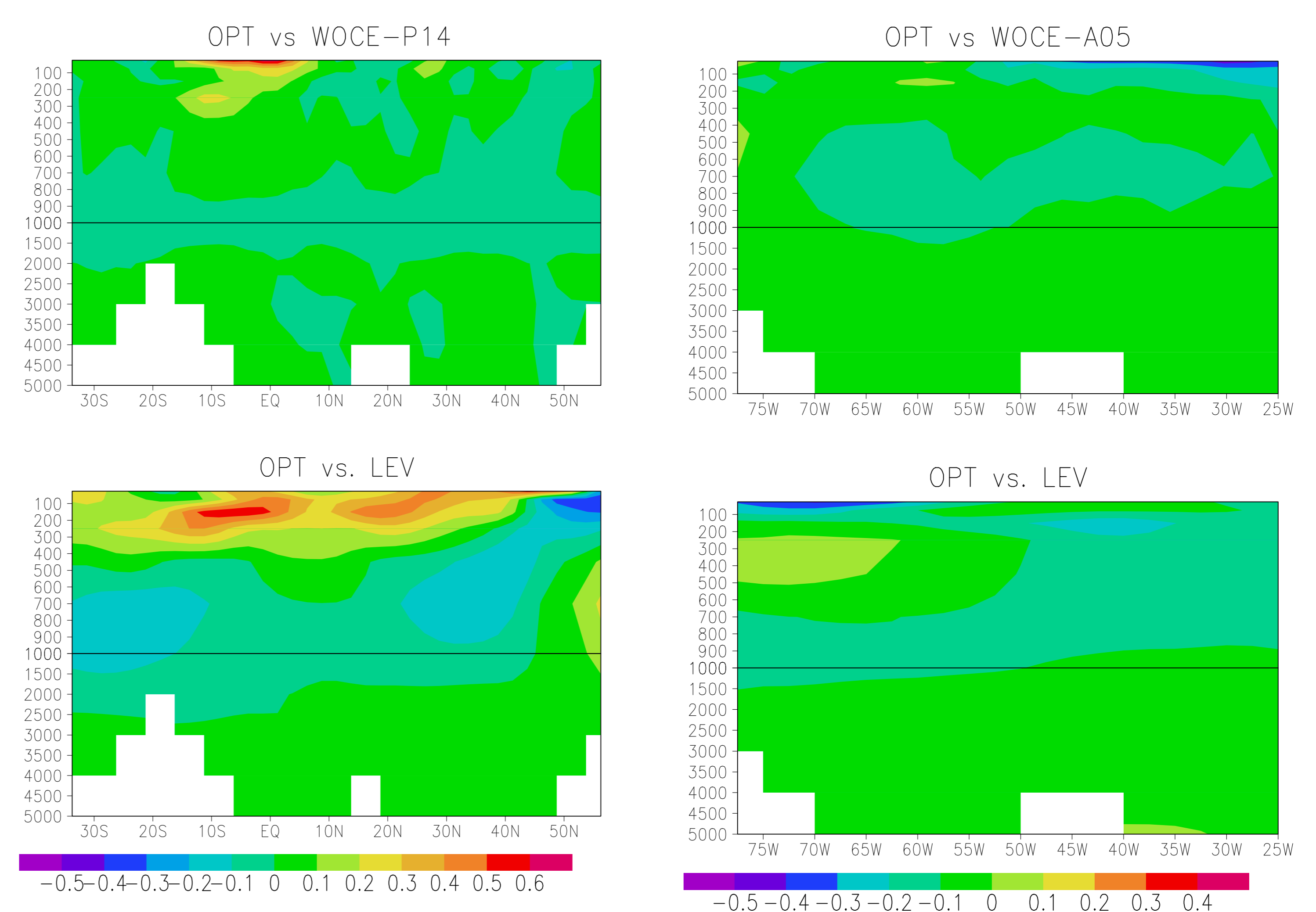


Time series of the volume transport along the ACC from the nine year optimal solution **OPT**.



A comparison of depth-latitude section of temperature ($^{\circ}$ C) taken at 180° W across Pacific and time averaged between July and September for: (top) differences between the model simulations and WOCE data and (bottom) differences between the model simulations and Levitus data.

A comparison of depth-longitude section of temperature ($^{\circ}$ C) taken at 24.5° N across Atlantic and time averaged between July and August for: (top) differences between the model simulations and WOCE data and (bottom) differences between the model simulations and Levitus data.



A comparison of depth-latitude section of salinity [psu] taken at 180° W across Pacific and time averaged between July and September for: (top) differences between the model simulations and WOCE data and (bottom) differences between the model simulations and Levitus data.

A comparison of depth-longitude section of salinity [psu] taken at 24.5° N across Atlantic and time averaged between July and August for: (top) differences between the model simulations and WOCE data and (bottom) differences between the model simulations and Levitus data.

Summary and Conclusions

- ⇒ The main aim of this study is to investigate the variability of the oceanic state in the last decades using 4D-variational data assimilation. We demonstrated that the combination of the ocean observations with models is beneficial for the global ocean analyses. The assimilation significantly improved the global ocean state.
- ⇒ It is clearly seen that the temporal evolution of the sea level height from the constrained model **OPT** is closer to observations than the reference run. The correlation of the sea level height between the model and T/P data is significantly improved in **OPT**.
- ⇒ A cross-comparison of the hydrographic data, T/P altimetry and the independent observations from the Tropical Atmosphere Ocean (TAO) mooring array revealed that the assimilation is capable to compensate for some model deficiencies.
- ⇒ The temporal mean Atlantic and Pacific heat and freshwater transports fit well to the data. The analyses revealed strong interannual variability.
- ⇒ Further constraining the model with higher resolution and addition of new data will be the next step.

References

- Hsiung J. (1985). Estimates of global meridional heat transport, *J. Phys. Ocean.*, *15*, 1405–1413.
- Macdonald A.M. (1995). Oceanic fluxes of mass, heat and freshwater: a global estimate and perspective. PhD thesis, MIT, Cambridge 02139
- Schlitzer R. (1993). Determining the mean large-scale circulation of the Atlantic with the adjoint method. *J. Phys. Ocean.*, *23*, 1935–1952.
- Talley L.D. (1984). Meridional heat transport in the Pacific Ocean, *J. Phys. Ocean.*, *14*, 231–241.
- Staneva J., M. Wenzel and J. Schröter (2002). Oceanic state during 1993–1999 determined by 4D VAR data assimilation, *International WOCE Newsletter*, *42*, 11–13.
- Wenzel, M., J. Schröter and D. Olbers (2001). The annual cycle of the global ocean circulation as determined by 4D VAR data assimilation. *Progr. in Oceanogr.*, *48*, 73–119.
- Wijffels S.E., R.W. Schmitt, H.L. Bryden and A. Stigebrandt (1992). Transport of freshwater by the ocean, *J. Phys. Ocean.*, *22*, 155–162.